

Fig. 4 Comparison of experimentally determined propane-air flame speeds from this and Parks investigations.

Results and Discussion

When the combustible mixture in the tube with the nozzle and and screen in place was ignited by the electrodes, a flat flame was generated. After ignition the generated flame propagated about 100 mm down the tube, the flame flattened out and propagated another 400 mm, at which point the flat shape was lost. Figure 2 shows a multiexposure photograph of the flame propagation taken with a sector disk shutter. From the experiments, it was found that a combination of screen mesh, screen location, and nozzle diameter generated the flat flame as shown in Table 1. Figure 3 shows the results of propane-air flame speed measurements. The delta-marked curve shows the results of the ion probe measurements and the circle-marked curve those of photomeasurement. In Fig. 4, curve 1 is from the work of Parks and curve 2 was obtained in the present study. The speeds of curves 1 and 2 differ by 2-3%. Curve 1 of Fig. 4 shows a small difference compared with curve 2, reflecting the influence of the temperature. Curve 1 was obtained at about a temperature of 20°C. In this study, the experiments were done at an atmospheric temperature of 7°C. Generally, the flame speed increases with increasing temperature, so a temperature correction was made. With correction, curve 2 almost agrees with curve 1. When the flame gets farther from the screen, the velocity-flattening action in the tube is lost, the intervals of flat flame propagation become a smaller fraction of the total propagation time. And, the flat flames are no longer stable.

Conclusions

This Note describes a new technique to measure the flame propagation rate in a cylindrical tube. It includes useful and interesting results that might be helpful to other researchers.

References

- ¹Fristrom, R. M., "The Determination of Fundamental Burning Velocities of Hydrocarbons by a Revised Tube Method," *Physics of Fluids*, Vol. 8, 1965, p. 273.
- ²Coward, H. F. and Hartwell, F. J., *Journal of the Chemical Society*, 1932, pp. 1996, 2676.
- ³Gerstein, M., Levine, O., and Wong, E. L., *Journal of the American Chemical Society*, Vol. 73, 1951, p. 418.
- ⁴Fuller, L. E., Parks, D. J., and Fletcher, E. A., "Flat Flames in Tubes—Easy Fundamental Flame Speed Measurements," *Combustion and Flame*, Vol. 13, 1969, p. 455.

An Approximation of the Lowest Eigenfrequencies and Buckling Loads of Cylindrical and Conical Shell Panels Under Initial Stress

Detlef Teichmann*

University of the Federal Armed Forces
Munich, Federal Republic of Germany

Introduction

THE vibrations of cylindrical and conical shells have been treated in a large number of publications¹ as have the vibrations of cylindrical shells and shell panels subjected to axial compression.² But only a few papers deal with the vibrations of conical shell panels under initial stress.³

The exact calculation of the eigenfrequencies of a shell requires, in most cases, a large amount of numerical computation. It is advantageous to the engineer to be able to study the influence of the most important parameters with a simple approximation, before he goes through expensive calculations. In this Note, an approximation formula for the calculation of vibrations of conical shells under initial stress will be derived.

Shell Equations

The equations of motion for thin, shallow shells (Donnell-Mushtari-Koiter) under initial stress are

$$\nabla_{\alpha} N^{\alpha\beta} + p^{\beta} = \rho h \ddot{u}^{\beta}$$

$$b_{\alpha\beta} N^{\alpha\beta} + \nabla_{\alpha} (\dot{N}^{\alpha\beta} \nabla_{\beta} w) + \nabla_{\alpha} \nabla_{\beta} M^{\alpha\beta} = \rho h \ddot{w} \quad (1)$$

with the boundary conditions

$$u_{\beta} = 0, \text{ or } n_{\alpha} N^{\alpha\beta} = 0$$

$$w = 0, \text{ or } n_{\alpha} (\nabla_{\beta} M^{\alpha\beta} + \dot{N}^{\alpha\beta} \nabla_{\beta} w) = 0$$

$$\nabla_{\beta} w = 0, \text{ or } n_{\alpha} M^{\alpha\beta} = 0 \quad (2)$$

$M^{\alpha\beta}$, $N^{\alpha\beta}$, $\dot{N}^{\alpha\beta}$ denote the tensors of the moment, force, and initial force resultants; p^{β} , p the surface loads; \ddot{u}^{β} , \ddot{w} the tangential and normal accelerations; $b_{\alpha\beta}$ the tensor of curvature; n_{α} the components of direction vector; ρ the mass density; h the shell thickness, and ∇_{α} the covariant differentiation symbol.

Cylindrical Shell Panel

For the vibrations of a cylindrical shell loaded only by normal stress in the direction of the generator (axial compression) and whose tangential inertia terms are neglected, one obtained from Eqs. (1) the well-known differential equations

$$r^2 u_{,ss} + \frac{1-\nu}{2} u_{,\theta\theta} + \frac{1+\nu}{2} r v_{,s\theta} + \nu r w_{,s} = 0$$

$$\frac{1+\nu}{2} r u_{,s\theta} + \frac{1-\nu}{2} r^2 v_{,ss} + v_{,\theta\theta} + w_{,\theta\theta} = 0$$

$$-\nu r u_{,s} - v_{,\theta} - w - \frac{h^2 r^2}{12} \Delta \Delta w + \frac{\dot{N}_{ss}}{B} r^2 w_{,ss} = r^2 \frac{\rho h}{B} \ddot{w} \quad (3)$$

Received July 27, 1983. Copyright © American Institute of Aeronautics and Astronautics, Inc., 1985. All rights reserved.

*Doctor of Engineering, Department of Aerospace Engineering.

where s is the coordinate in the direction of the generator, ϑ the coordinate of the circumferential direction, r the radius of the cylindrical shell, and $B = Eh/(1 - \nu^2)$ the strain stiffness. With the assumed displacement functions

$$\begin{aligned} u(s, \vartheta, t) &= C_u \cos[j\pi(s/l)] \sin[n\pi(\vartheta/\gamma)] \sin(\omega t + \varphi) \\ v(s, \vartheta, t) &= C_v \sin[j\pi(s/l)] \cos[n\pi(\vartheta/\gamma)] \sin(\omega t + \varphi) \\ w(s, \vartheta, t) &= C_w \sin[j\pi(s/l)] \sin[n\pi(\vartheta/\gamma)] \sin(\omega t + \varphi) \end{aligned} \quad (4)$$

the differential equations (3) can be integrated immediately for the special case of a cylindrical shell panel, which is supported at all four edges by shear diaphragms (SS-3 boundary condition). An equation is yielded for the eigenvalues $\lambda(j, n) = \omega^2(j, n)r^2\rho h/B$. C_u , C_v , C_w are constants, ω is the angular frequency, t denotes the time, and φ is the phase angle.

In vibration and stability problems, the mode shapes of shells of revolution show many half-waves in the circumferential direction. By minimizing λ with respect to the number of the circumferential half-waves n , the following minimal eigenvalues are yielded

$$\lambda^{\min}(j) = \left(\frac{\dot{N}_{ss}}{B} + \sqrt{\frac{1-\nu^2}{3}} \frac{h}{r} \right) \left(j\pi \frac{r}{l} \right)^2 \quad (5)$$

The limit of stability is reached when the eigenfrequency disappears. Then one obtains the classical buckling stress for the cylindrical shell subjected to axial compression, which also holds for the spherical shell loaded by external pressure

$$\delta_{crit}^{\dot{N}_{ss}} = -\frac{E}{\sqrt{3(1-\nu^2)}} \frac{h}{r} \quad (6)$$

Approximation for Conical Shells

No analytic solution can be given for the differential equations of conical shells. With the hypothesis of local buckling, however, Eq. (5) can be extended in such a way that it also holds, by approximation, for conical shells and cylindrical shells with other boundary conditions. The hypothesis says that the buckling instability is determined by the stress state and the momentary shape of the shell inside the zone of the initial buckle.⁴ If one applies this hypothesis also to the mode shapes of vibrations, because of the similarity of vibration and stability problems, and substitutes in Eq. (5) the normal stress $\dot{\sigma}$ and the radius r of the cylindrical shell by the normal stress $\dot{\sigma}_u$ and the main curvature radius $a/\cos\alpha$ on the lower edge of the conical shell (see Fig. 1), a simple formula is yielded for calculating the smallest eigenfrequencies ω and the smallest buckling stress $\dot{\sigma}_u^{crit}$ of conical shells.

$$\omega_{(j)}^{\min} = \sqrt{\frac{\dot{\sigma}_u}{E} + \frac{1}{\sqrt{3(1-\nu^2)}} \frac{h}{a} \cos\alpha} \sqrt{\frac{E}{\rho}} (j+k) \frac{\pi}{l} \quad (7)$$

The circumferential included angle γ , the half-wave number n , and the boundary conditions in the circumferential direction are not included in this equation because the eigenfrequency has been minimized with respect to the number of circumferential half-waves.

To the number of half-waves j in the direction of the generator, a correction factor k was added, which allows consideration of different boundary conditions on the upper and lower edges of the conical shell (e.g., similar to a beam for the normal displacement w : $k=0$ for simply supported; $k=0.25$ for clamped-simply supported; $k=0.5$ for clamped-clamped).

Discussion of Results

To check approximation formula (7), the eigenfrequencies and mode shapes of different conical shell panels under initial stress were more accurately calculated.³ The partial differential equations (1) were substituted by a two-dimensional finite difference method; the eigenvalue problem was solved with the aid of a QR-algorithm. As examples, the approximate solutions (7) in Figs. 2a, 3a, and 4a are compared to the more accurate calculations shown in Figs. 2b, 3b, and 4b.

The eigenvalues $\lambda = \omega^2 a^2 \rho h/B$ are plotted vs the compression $q = -10^3 \dot{\sigma}_u h/B$. Each straight line belongs to a mode shape. The numbers (j, n) indicate the number of half-waves of the mode shape in the direction of the generator and in circumferential direction. Straight lines with an equal number of half-waves in the direction of the generator are running almost parallel. There is a linear relationship between the squares of the eigenfrequencies and the load. The eigenvalues decrease with increasing compression; they disappear if the critical load for this mode shape has been reached. This allows the buckling load for a mode shape to be determined by two frequency measurements under different loads without subjecting the structure to the destructive critical load.

Figures 2a and 2b apply to a conical shell panel supported by shear diaphragms (SS-3) at all edges. The approximate solutions for the lowest eigenvalues with $j=1, 2, 3$ half-waves in the direction of the generator converge with the growth of q , giving the same buckling load ($q=7.1$). In Fig. 2b one sees that the mode shape (1,3) has the lowest eigenfrequency. The comparison of the two diagrams shows that—with the aid of approximation formula (7)—the lowest eigenvalues can be obtained with reasonable accuracy.

Figures 3a and 3b indicate the eigenvalues of a conical shell segment clamped at all edges without axial constraint (C-3). In this example, the lowest eigenvalues belong to mode shapes with few half-waves in the circumferential direction (1,2)/(2,2)/(3,2), because the included angle ($\gamma=45$ deg) is small. But the influence of the edges is still not very large, thus Eq. (7) provides good results, even in this case.

Figures 4a and 4b describe the dependence of the eigenvalues on the vertex half-angle α for a shallow conical shell whose inside edge is clamped without axial constraint (C-3), the outside edge is fully clamped (C-4), and the straight

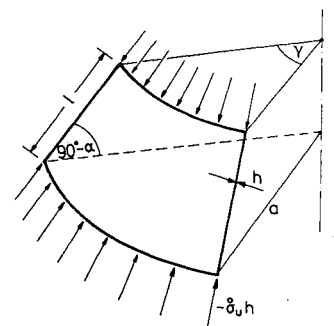
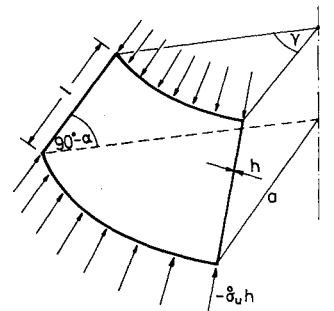


Fig. 1 Conical shell panel.



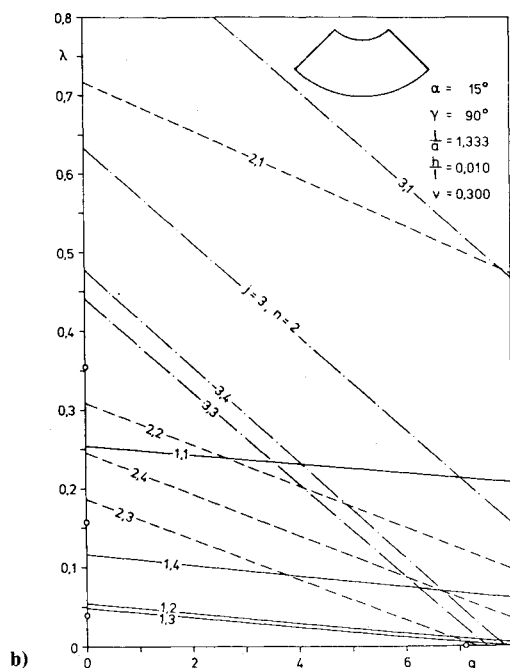
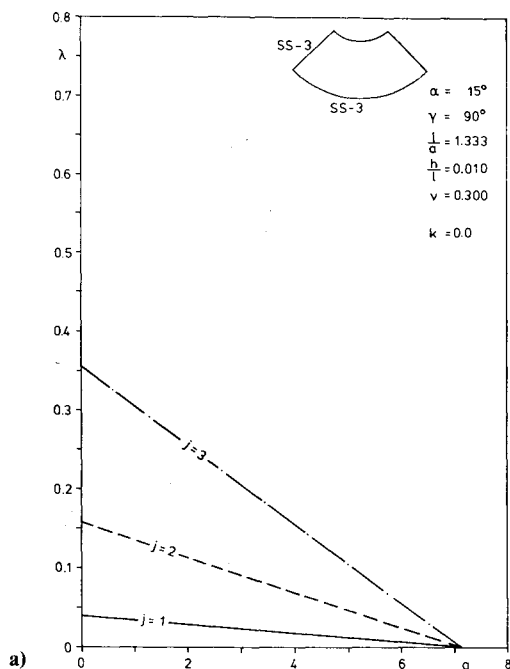


Fig. 2 Eigenvalues λ of a simply supported (SS-3) conical shell panel as a function of compression q .

edges are supported by shear diaphragms (SS-3). In the case of this half-conical shell, the vertex half-angle is enlarged until the shell becomes a circular ring plate. The compression ($q=0.2$) remains constant. In the case of the plate ($\alpha=90$ deg), the mode shape (1,1) has the lowest eigenfrequency. But even a small curvature—i.e., a vertex half-angle of less than 86 deg—changes the sequence of the eigenfrequencies for the mode shapes with one half-wave in the direction of the generator. In the case of mode shapes with two half-waves in the direction of the generator, the sequence changes at about 78 deg. Equation (7) is not valid for the transition to the circular plate. In this example it becomes zero for $\alpha=86$ deg because, contrary to a shell of revolution, the mode shapes for the lowest eigenvalues of plates have no local (small) buckles.

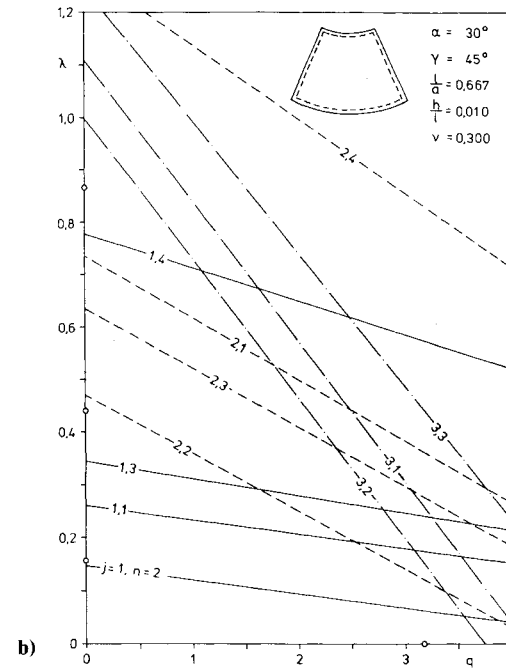
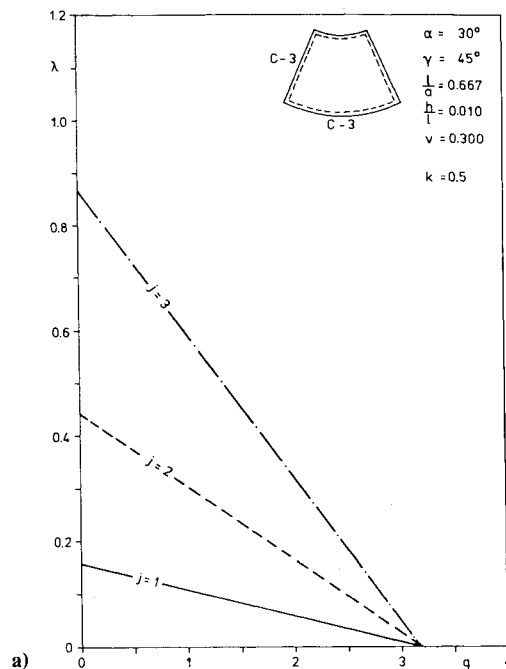


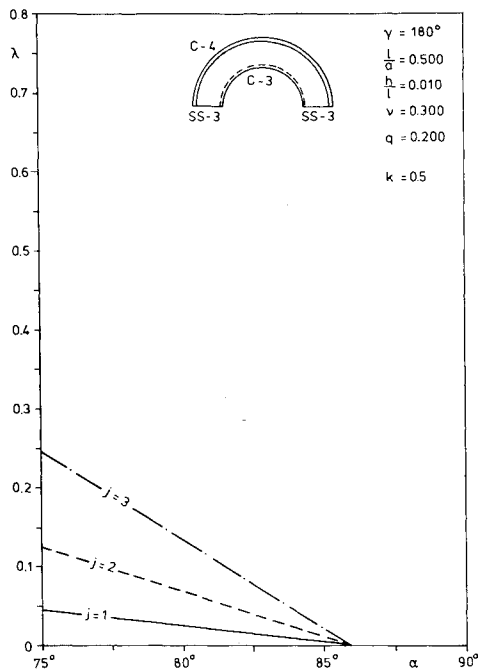
Fig. 3 Eigenvalues λ of a clamped (C-3) conical shell panel as a function of compression q .

To give a better idea, a few mode shapes of conical shell panels are depicted in Figs. 5a-c. Figure 5a shows the mode shape (2,3) of the conical shell from Figs. 2a and 2b; Fig. 5b shows the mode shape (3,2) of the conical shell from Figs. 3a and 3b; and Fig. 5c shows the mode shape (1,5) of the conical shell from Figs. 4a and 4b.

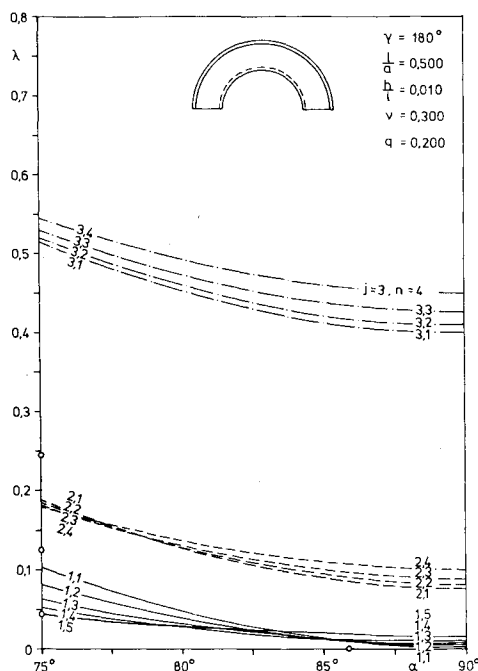
To demonstrate the vibration behavior of these conical shell panels with increasing compression, a 5-minute computer-trickfilm has been made by the author.

Summary

The solution for the lowest eigenfrequencies of a cylindrical shell panel, simply supported at all four edges, under axial compression, is extended by the hypothesis of local buckling to an approximation formula for conical shell



a)



b)

Fig. 4 Eigenvalues λ of a shallow conical shell as a function of vertex half-angle α .

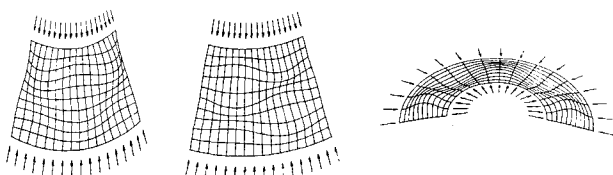


Fig. 5 Mode shapes of conical shell panels under compression.

panels with different boundary conditions. Comparison with more accurate numerical calculations shows that the approximation gives good results for the frequency- and load-range in which a conical shell neither vibrates in resonance nor buckles.

References

- ¹Leissa, A. W., "Vibration of Shells," NASA SP-288, Washington, DC, 1973.
- ²Singer, J., Rand, O., and Rosen, A., "Vibrations of Axially Loaded Stiffened Cylindrical Panels with Elastic Restraints," Dept. of Aeronautical Engineering, Technion—Israel Institute of Technology, Haifa, TAE 439, 1981.
- ³Teichmann, D., "Vibrations of Preloaded Conical Shell Segments," Dissertation, Hochschule der Bundeswehr München, 1982 (in German).
- ⁴Axelrad, E. L., "On Local Buckling of Thin Shells," Collection of Papers of the 25th Israel Annual Conference on Aviation and Astronautics, Haifa, 1983, pp. 285-292.

Static Instability of an Elastically Restrained Cantilever Under a Partial Follower Force

Lech Tomski* and Jacek Przybylski†
Czestochowa Institute of Technology
Czestochowa, Poland

Introduction

THE stability of a cantilever under a force influenced by a parameter η (see Fig. 1) was examined by Dzhaneldze.¹ He found that, particularly within the range $0 \leq \eta \leq 0.5$, the static criterion of instability remains valid, i.e., the loss of stability occurs by divergence and not by flutter. Sundararajan² considered a uniform, clamped, elastically supported column subjected to a tangential load at the elastically supported end. He found that the critical instability mechanism changed from flutter to divergence, or vice versa, with a change in the stiffness of the elastic supports. Kounadis³ considered simple structure elastically restrained under follower compressive forces. He pointed out that the type of instability in the structures is also dependent on the values of the constants of elastic restraint. In Ref 4, Kounadis presented a thorough discussion of the influence of the parameters of the elastic end constraints on the type of instability and estimated the smallest critical load of a column under tangential compressive force using a static stability criterion. The stiffness constant of a rotational or translational spring at one end of the column was assumed to be a parameter.

In this Note, the influence of the follower parameter η and an elastic end support on the divergence instability of the column will be investigated. The divergence instability of the column mentioned above subjected to the load changing from a constant direction ($\alpha = 0$) to a purely tangential one ($\alpha = 1$), is taken into consideration. The basic analytical method used by Kounadis⁴ has been adopted here.

Received June 27, 1984; revision received Oct. 8, 1984. Copyright © American Institute of Aeronautics and Astronautics, Inc., 1984. All rights reserved.

*Associate Professor, Department of Mechanics and Machine Design Foundations.

†Senior Assistant, Department of Mechanics and Machine Design Foundations.